Scientia Iranica, Vol. 10, No. 4, pp 419–425

SCIENTIA
IRANICA

Variational Finite Element Method for Axisymmetric Magneto-Hydrodynamic Equilibrium

F. Dini[1], S. Khorasani[2] and R. Amrollahi*

In this paper, a new formalism of the finite element method is presented which is capable of analyzing axisymmetric magneto-hydrodynamic plasma equilibrium through the variational formulation of the Grad-Shafranov equation. Several problems in terms of the integrands and suspicious boundary conditions are encountered and successfully removed. Detailed theoretical and numerical considerations are presented and the results of the method are compared to the results from an exact code based on the Green function technique.

INTRODUCTION

The numerical solution of the Grad-Shafranov equation, which describes axisymmetric plasma equilibrium, has been reported through various methods [1-3] including the finite difference method, inverse variables, moments method, method of eigenfunctions, Green function method and finite element method. Numerical determination of axisymmetric toroidal magneto-hydrodynamic equilibrium has been reported by the application of iterative schemes [4] and exact [5] and approximate [6] variational moment methods. Free-boundary plasma equilibrium in axisymmetric tori has also been considered by a combination of alternating direction implicit and iterative methods [7], as well as integral transform techniques [8]. Variational approaches have been exploited to discuss the solution [9] and existence of free boundary solutions of the Grad-Shafranov equation [10]. Also, free boundary field-reverse configurations of plasma equilibrium have been analyzed by means of the boundary element method [11]. None of the mentioned methods is, however, as versatile and powerful as the finite element method [12,13], because of its flexibility to adapt arbitrary geometries and its reasonable efficiency and error distribution.

Classes of the finite element method fall into two major categories [13]: The Galerkin and the variational method. In both approaches the solution is expanded on a set of eigenfunctions. However, in the Galerkin method, the coefficients are found through an integral equation while in the variational approach the coefficients are found through extremization of an equivalent integral. Besides the simplicity of variational finite elements, it permits accurate evaluation of solution functions so that in the limit of small elements, the solution should converge to the exact analytical one [12]. The variational approach of finite elements is superior in terms of error distribution, when compared to the Galerkin methods, since as a special case of the moments method, the variational finite elements are equivalent to a least-square minimization of error [13]. Also, variational formulations of finite elements lead to a symmetric sparse coefficients matrix, resulting in considerable improvements in code efficiency and storage considerations.

Galerkin finite elements have been extensively used in computation of closed-boundary and free-boundary plasma equilibrium [14]. However, in the adaptation of variational finite elements to axisymmetric plasma equilibrium, numerous problems arise. Part of these problems is due to an artificial boundary condition of either a Dirichlet or Neumann type in the solution. To the best knowledge of the authors, no

1. *Department of Physics, Amir Kabir University of Technology, Tehran, I.R. Iran.*
2. *Department of Plasma Physics, AEOI, P.O. Box 14155-1339, Tehran, I.R. Iran.*
*. *Corresponding Author, Department of Physics, Khaje Nassir-Al-Dean Toosi University of Technology, Tehran, I.R. Iran.*

report has considered a variational formulation of finite elements for this purpose.

Here, a successful implementation of variational finite elements is presented based on first-order triangular meshes by locating and removing the above problems in the theoretical description of the finite element method. The method is verified by comparing the results corresponding to a quadruple axisymmetric configuration obtained through the Green function technique [15]. The developed equilibrium code has been used to simulate the time-domain, self-consistent plasma equilibrium in Tokamak [16].

AXISYMMETRIC VARIATIONAL FINITE ELEMENTS

The Grad-Shafranov equation, which describes the axisymmetric plasma equilibrium reads [3]:

$$\frac{1}{r}\Delta^*\Psi = -\mu_0 J_t, \tag{1}$$

in which Ψ is the poloidal magnetic flux, J_t is the toroidal current density, which includes contributions from the toroidal current densities of plasma and poloidal coils and Δ^* is the elliptic Grad-Shafranov operator;

$$\Delta^* = r\frac{\partial}{\partial r}\left(\frac{1}{r}\frac{\partial}{\partial r}\right) + \frac{\partial^2}{\partial z^2} = \frac{\partial^2}{\partial r^2} - \frac{1}{r}\frac{\partial}{\partial r} + \frac{\partial^2}{\partial z^2}, \tag{2}$$

where r and z are the radial and longitudinal coordinates in the cylindrical system of coordinates, respectively (obviously, this operator differs from the Laplacian operator in axisymmetric cylindrical coordinates). It can be easily shown that Equation 1 may be regarded as the Euler-Ostogradskii equation [17] of the functional [6,8,16]:

$$\Pi(\Psi) = \iint \left(\frac{1}{2r}|\nabla\Psi|^2 - \mu_0 J_t \Psi\right) dr dz. \tag{3}$$

Here, the gradient operator is given in cylindrical coordinates as $\Delta = \partial/\partial r\hat{r} + \partial/\partial z\hat{z}$ and the integration is taken over a two-dimensional solution region in (r, z), whose volume of revolution about the z-axis generates the original three-dimensional system, as illustrated in Figure 1.

In the finite element method, the solution region is discretized into small non-overlapping elements and in each element a pre-assumed form for the unknown is taken, being a function of coordinates and fixed triangle vertices. These vertices, being referred to as nodes, are usually shared by more than one element and it is desirable to find the nodal values of the unknown functions through a set of algebraic operations which simultaneously extremize Equation 3.

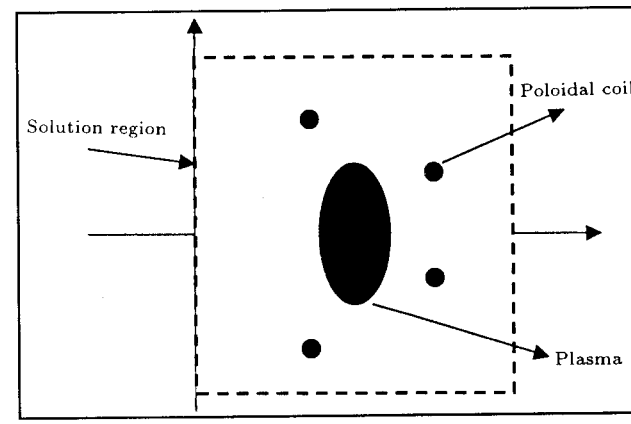

Figure 1. Typical solution region; the original three-dimensional region is generated by revolution about z-axis.

If the elements were chosen to be triangles, then the variations of the discretized function over the element e would be linear, so that:

$$\Psi^e(r, z) = a^e + b^e r + c^e z, \tag{4}$$

in which the e superscript refers to the element e and constants a, b and c are determined from:

$$\begin{bmatrix} a^e \\ b^e \\ c^e \end{bmatrix} = \begin{bmatrix} 1 & r_i^e & z_i^e \\ 1 & r_j^e & z_j^e \\ 1 & r_k^e & z_k^e \end{bmatrix}^{-1} \begin{bmatrix} \Psi_i \\ \Psi_j \\ \Psi_k \end{bmatrix} \equiv \mathbf{D}^e \boldsymbol{\Psi}^e. \tag{5}$$

Here, the i, j and k subscripts refer to the indices of the three nodes belonging to the element e and r_l^e and z_l^e correspond to the radial and longitudinal coordinates of the node l, belonging to the element e with l standing for i, j or k. This special way of discretization of the unknown function results in a continuous form over the entire solution region, while maintaining simple linear form of Equation 4 over each individual element.

It is customary to define the shape functions $\mathbf{N}_l^e, l = i, j$ or k, for the element e as:

$$\mathbf{N}^e(r, z) \equiv \begin{bmatrix} \mathbf{N}_i^e(r, z) \\ \mathbf{N}_j^e(r, z) \\ \mathbf{N}_k^e(r, z) \end{bmatrix} \equiv \mathbf{D}^{e^T} \begin{bmatrix} 1 \\ r \\ z \end{bmatrix}, \tag{6}$$

so that one has:

$$\Psi^e(r, z) = \mathbf{N}^{e^T}(r, z)\boldsymbol{\Psi}^e. \tag{7}$$

Therefore, the gradient of the unknown function over element e may be approximated as:

$$\nabla\Psi^e = \nabla\mathbf{N}^{e^T}\boldsymbol{\Psi}^e = \begin{bmatrix} D_{ji}^e & D_{jj}^e & D_{jk}^e \\ D_{ki}^e & D_{kj}^e & D_{kk}^e \end{bmatrix} \boldsymbol{\Psi}^e \equiv \mathbf{B}^e\boldsymbol{\Psi}^e, \tag{8}$$

where, D_{rs}^e refer to the elements of the matrix $\mathbf{D}^e$.

Plugging Equations 7 and 8 into Equation 3 gives:

$$\Pi(\Psi) \approx \sum_e \Pi^e(\Psi^e)$$

$$= \sum_e \iint_{S^e} \Big(\frac{1}{2r} \Psi^{e^T} \mathbf{B}^{e^T} \mathbf{B}^e \Psi^e$$

$$- \mu_0 \mathbf{J}_t^{e^T} \mathbf{N}^{e^T} \mathbf{N}^e \Psi^e \Big) dr dz, \tag{9}$$

in which the summation is done over all elements and $\mathbf{J}_t^e$ is the array of nodal values of the toroidal current density function J_t over the i, j and k nodes of element e; in this way, J_t is discretized into piece-wise linear functions similar to Equation 4. Also, S^e denotes the area occupied by element e. The numerical value of the area of an element is obtainable from:

$$S^e = \frac{1}{2} \left| \det(\mathbf{D}^e) \right|^{-1}. \tag{10}$$

The variational property of Equation 3 requires that the functional Equation 9 be stationary, with respect to array Ψ of the nodal values of the unknown function. Hence:

$$\frac{\partial}{\partial \Psi^e} \sum_e \Pi^e(\Psi^e) = 0, \tag{11}$$

which turns into the set of linear algebraic equations:

$$\sum_e \iint_{S^e} \frac{1}{r} dr dz \mathbf{B}^{e^T} \mathbf{B}^e \Psi^e = \mu_0 \sum_e \iint_{S^e} \mathbf{N}^{e^T} \mathbf{N}^e dr dz \mathbf{J}_t^e. \tag{12}$$

Now, the partial stiffness matrix $\mathbf{K}^e$ is defined and the partial force vector $\mathbf{F}^e$ is defined as:

$$\mathbf{K}^e = \iint_{S^e} \frac{1}{r} dr dz \mathbf{B}^{e^T} \mathbf{B}^e, \tag{13a}$$

$$\mathbf{F}^e = \mu_0 \iint_{S^e} \mathbf{N}^{e^T} \mathbf{N}^e dr dz \mathbf{J}_t^e \equiv \mu_0 \mathbf{E}^e \mathbf{J}_t^e. \tag{13b}$$

Here, it can be observed that the 3×3 square matrices $\mathbf{K}^e$ and $\mathbf{E}^e$ are symmetric. Fortunately, there are simple closed form expressions for evaluation of $\mathbf{E}^e$ [12,13]. Also the double integral in $\mathbf{K}^e$ can be directly evaluated through algebraic expansion of the integral region. A general approach for algebraic evaluation of integrals arising in axisymmetric finite element problems has been reported [18]. For instance, the basic triangular elements of A- and B-type, as shown in Figure 2a, lead to the following expressions:

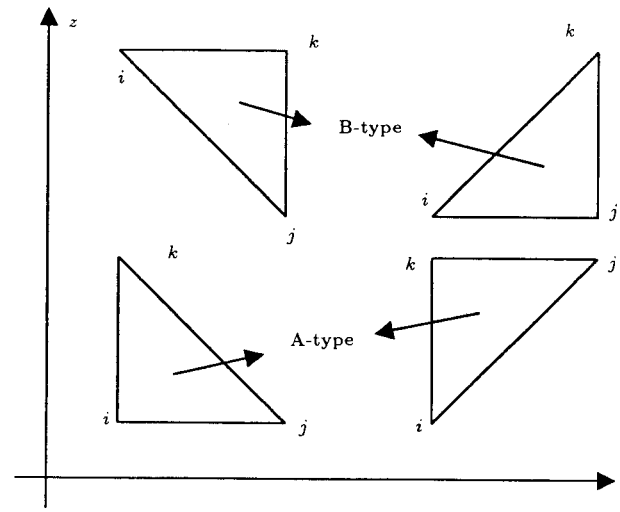

Figure 2a. Illustration of elementary triangular meshes of A- and B-type.

$$\iint_{S^e} \frac{1}{r} dr dz = (z_k - z_i) \left[\frac{r_j}{r_j - r_i} \ln \frac{r_j}{r_i} - 1 \right],$$

for A-type element, (14a)

$$\iint_{S^e} \frac{1}{r} dr dz = (z_k - z_j) \left[\frac{r_i}{r_i - r_j} \ln \frac{r_j}{r_i} + 1 \right],$$

for B-type element. (14b)

For other triangular elements not being of the elementary forms presented in Figure 2a, combinations of A-type and B-type elements can always be used. Any triangular element can be set in a rectangle, with three A or B type triangles remaining as illustrated in Figure 2b. Hence, by subtraction of the integrals belonging to the basic type elements from the surface integral on the rectangle, which is simply known, the unknown surface integral of the triangle is found. Therefore, there is no need for numerical integration

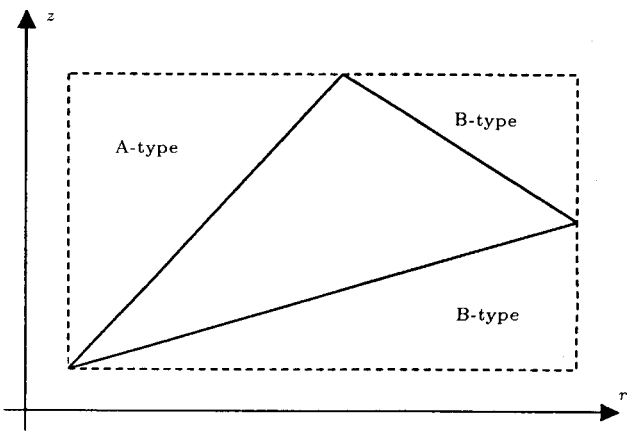

Figure 2b. Enclosing an arbitrary triangle in a rectangle with the aid of basic A- and B-type elements.

to build up the final system of equations and efficient evaluation of Equation 13 is always possible.

Hence, the system of Equation 12 can be rewritten as:

$$\mathbf{K}\Psi = \mathbf{F}, \tag{15}$$

where the overall stiffness matrix, $\mathbf{K}$, and force vector, $\mathbf{F}$, have the dimensions $N \times N$ and $N \times 1$ (N being the total number of nodes), respectively and are generated by superposition of the corresponding partials, as given by Equation 13. The $N \times 1$ vector, $\Psi = \mathbf{K}^{-1}\mathbf{F}$, also denotes the array of unknown nodal values of the poloidal flux function.

It is easy to check that the stiffness matrix, $\mathbf{K}$, is sparse and, therefore, little storage is needed to store its non-zero elements. Also, it is symmetric with respect to its major diagonal and, thus, approximately half of the above storage would suffice to uniquely determine $\mathbf{K}$. The process of inversion of $\mathbf{K}$ can be achieved through standard inversion techniques, however, the best one is to employ the so-called iterative gradient techniques [13]. The gradient techniques are more efficient than other approaches for solution of linear simultaneous equations, considerably for typical matrix dimensions of 1000 and over and, more importantly, result in uniform error distribution. More specifically, the conjugate-gradient method reaches the exact solution (within the truncation round-off errors) in, at most, N iterations for elliptic problems.

However, the above point is not the end of the story and, in general, Equation 15 leads to erroneous results as discussed in the next section.

PROBLEMS WITH THE FORMULATION

Singularity of Equation 15

At the first look, the set of linear algebraic Equations 15 cannot be solved, since the stiffness matrix, $\mathbf{K}$ is singular. This is due to the fact that according to Equation 1, the Grad-Shafranov equation is insensitive to the choice of a reference for Ψ. Therefore, some nodes must be subject to a boundary condition of the Dirichlet type, so that $\mathbf{K}$ is not singular. It is now shown that Ψ must take on zero value on the z-axis.

In general, the Grad-Shafranov equation has Green function solutions of the following form:

$$\Psi(r,z) = \mu_0 \int_{-\infty}^{\infty}\int_{0}^{\infty} G(\mathbf{r},\mathbf{r}')J_t(\mathbf{r}')r'dr'dz', \tag{16}$$

in which $\mathbf{r} = r\hat{r} + z\hat{z}$ and $G(\mathbf{r},\mathbf{r}')$ is the Green function of Equation 2 [15]:

$$G(\mathbf{r},\mathbf{r}') = \frac{\sqrt{rr'}}{2\pi} Q_{\frac{1}{2}}\left[1 + \frac{|\mathbf{r}-\mathbf{r}'|^2}{2rr'}\right]. \tag{17}$$

Here, $Q_{\frac{1}{2}}(x)$ is the Legendre function of the second kind. It is possible to show that Equation 17 has the asymptotic form near the z-axis [15]:

$$G(\mathbf{r},\mathbf{r}') \sim \frac{r^2 r'^2}{4[r^2 + r'^2 + (z-z')^2]^{\frac{3}{2}}}, \tag{18}$$

from which:

$$\lim_{r\to 0+} G(\mathbf{r},\mathbf{r}') = 0. \tag{19}$$

Accordingly, the poloidal flux function $\Psi(r,z)$ has to take on zero value at $r = 0$. This shows that a zero-boundary condition of the Dirichlet type over the symmetry axis exists, which reads:

$$\Psi(0,z) = 0. \tag{20}$$

It is necessary to insert this boundary condition into Equation 15 to avoid a singular coefficient matrix $\mathbf{K}$. Insertion of the boundary condition is possible through removing the nodes near the symmetry axis from Equation 15 and proper reduction of the order of equations.

Non-Physical Neumann Boundary Conditions

Another problem with the system of Equation 15, is the presence of a non-physical boundary condition of homogeneous Neuman type over the borders of the solution region. This difficulty arises in the form of normal magnetic surfaces or poloidal flux contours at the boundaries in the numerical solution. In mathematical representation, one observes that:

$$\frac{\partial}{\partial n}\Psi = 0, \tag{21}$$

in which n stands for the normal vector to the boundaries. Indeed, this boundary condition is imposed by the variational formulation of the Grad-Shafranov Equation 3, as explained below.

Taking the variation of Ψ in Equation 3 from both sides, one can show that:

$$\delta\Pi(\Psi) = \iint \left(\frac{1}{r}\nabla\Psi.\nabla\delta\Psi - \mu_0 J_t \delta\Psi\right) drdz. \tag{22}$$

Using the identity:

$$\frac{1}{r}\nabla\Psi.\nabla\delta\Psi = \nabla.\left(\frac{\delta\Psi}{r}\nabla\Psi\right) - \frac{\delta\Psi}{r}\Delta^*\Psi, \tag{23}$$

Equation 22 takes the following form:

$$\delta\Pi(\Psi) = -\iint \left(\frac{1}{r}\Delta^*\Psi + \mu_0 J_t\right)\delta\Psi drdz + \iint \nabla.\left(\frac{\delta\Psi}{r}\nabla\Psi\right) drdz. \tag{24}$$

The second integral in Equation 24 can be rewritten as:

$$\iint \nabla \cdot \left(\frac{\delta\Psi}{r}\nabla\Psi\right) drdz = \oint \frac{\delta\Psi}{r}\frac{\partial\Psi}{\partial n}ds, \tag{25}$$

where the contour integration is done in a counter-clockwise sense in the (r, z) plane.

Setting Equation 24 equal to zero requires that Equation 1 would hold. Therefore, in order to prevent the effect of Equation 25 entering the solution, either Ψ should be fixed over the boundary, that is the case only for the left boundary at $r = 0$ with Equation 20, or its normal derivate should vanish, as stated by Equation 21.

Physically, if the system is symmetric with respect to its equatorial plane at $z = 0$, the solution region can be halved at $z = 0$. In this case, Equation 21 must hold at the bottom of the solution region in order to maintain the mirror symmetry. However, the numerical solution over the right and upper borders would be meaningless, because of the fact that Equation 21 is here non-physical. To avoid this difficulty, the infinite elements [12] should be used over the upper and right boundaries (and the bottom boundary for asymmetric systems with respect to $z = 0$). The infinite elements virtually extend the solution region to infinity, where both Ψ and $\nabla\Psi$ tend to zero and, therefore, Equation 21 is satisfied.

A typical infinite element is illustrated in Figure 3. The definition of an infinite element relies on taking three fixed reference points, which are not in a straight line. The first point can be chosen to be the origin of the system of coordinates at (0,0). However, the second and third points vary with the position of the infinite element. In order to preserve the continuity of solution, it is necessary to choose two consecutive boundary nodes to serve as these two points, e.g. at (r_1, z_1) and (r_2, z_2).

The triangular system of coordinates (ρ, ξ) for the infinite element, e, are defined as:

$$r = \rho\Big[r_1^e + \xi(r_2^e - r_1^e)\Big], \tag{26a}$$

$$z = \rho\Big[z_1^e + \xi(z_2^e - z_1^e)\Big]. \tag{26b}$$

This coordinate transformation will be utilized for mapping the infinite element into a rectangular region, so that the infinite element, e, occupies the area extended from $\rho = 1$ to $\rho = \infty$ and from $\xi = 0$ to $\xi = 1$. This technique simplifies the evaluation of integrals. Moreover, the flux function is assumed to behave as:

$$\Psi^e(\rho, \xi) = \frac{1}{\rho}\Big[\xi\Psi_i^e + (1 - \xi)\Psi_j^e\Big], \tag{26c}$$

within the infinite element. This special definition of variation of the unknown function on the infinite element guarantees continuity of the solution on all three borders of the element, as well as decaying the solution and its derivative at infinity.

Now the contribution of the element integrals corresponding to the infinite elements should be added to Equation 12. Since $J_t = 0$ outside the solution region where the infinite elements are, therefore, the infinite elements only affect the stiffness matrix, $\mathbf{K}$. Therefore, it would only be necessary to compute the corresponding partial stiffness matrices, $\mathbf{K}^e$.

Following similar approaches to those presented in the previous section and changing the system of coordinates to the triangular system in the double integral, one can show that:

$$\mathbf{K}^e = \int_0^1\int_1^\infty \frac{1}{\rho\Big[r_1^e + \xi(r_2^e - r_1^e)\Big]}\mathbf{B}^{e^T}\mathbf{B}^e\frac{\partial(r, z)}{\partial(\rho, \xi)}d\rho d\xi, \tag{27}$$

in which the Jacobian of the triangular system of coordinates is given by:

$$\frac{\partial(r, z)}{\partial(\rho, \xi)} = 2A^e\rho. \tag{28}$$

Here, A^e is the area of the triangle formed by the three reference points. If the ordering of the reference points is not so that the corresponding triangle passes through them in a counter-clockwise sense, A^e should be chosen to be negative. This is because of the fact that A^e can be obtained indeed by matrix manipulations, where changing the order of rows changes the sign of a determinant, corresponding to the A^e. It can be noticed that the partial stiffness matrix is symmetric again.

Also, matrix $\mathbf{B}^e$, as a function of coordinates, is given by:

$$\mathbf{B}^e = \begin{bmatrix} \frac{\xi-1}{\rho}\frac{\partial\rho}{\partial r} - \frac{1}{\rho}\frac{\partial\xi}{\partial r} & -\frac{\xi}{\rho^2}\frac{\partial\rho}{\partial r} + \frac{1}{\rho}\frac{\partial\xi}{\partial r} \\ \frac{\xi-1}{\rho}\frac{\partial\rho}{\partial z} - \frac{1}{\rho}\frac{\partial\xi}{\partial z} & -\frac{\xi}{\rho^2}\frac{\partial\rho}{\partial z} + \frac{1}{\rho}\frac{\partial\xi}{\partial z} \end{bmatrix}. \tag{29}$$

Thus, the evaluation of the partial stiffness matrix needs numerical integration.

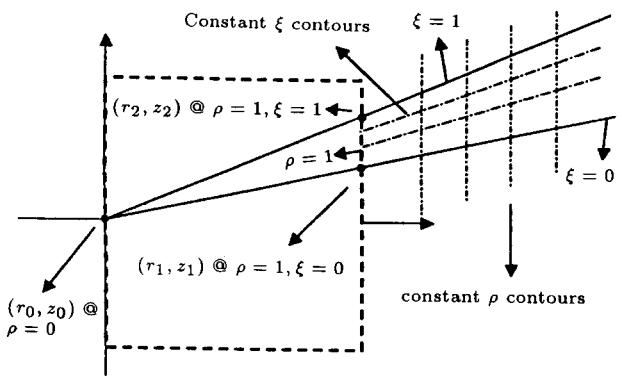

Figure 3. Infinite element used in the computation of magnetic poloidal flux.

RESULTS

In this section, the results of the computation of a developed, free-boundary equilibrium code are presented, which is based on the theoretical considerations above. Here, a magnetic quadruple is assumed with four magnetic coils at $(2, \pm 1)$ with the unit current outwards and $(1, \pm 2)$ with the unit current inwards. The cross-sectional dimensions of magnetic coils are supposed to be infinitely small. Therefore, the exact solution for the poloidal flux, according to Equations 16 and 17, would be:

$$\Psi(r,z) = \frac{\sqrt{r}}{2\pi} Q_{\frac{1}{2}} \left[\frac{r^2 + 1 + (z-2)^2}{2r} \right] + \frac{\sqrt{r}}{2\pi} Q_{\frac{1}{2}} \left[\frac{r^2 + 1 + (z+2)^2}{2r} \right] - \frac{\sqrt{r}}{\sqrt{2}\pi} Q_{\frac{1}{2}} \left[\frac{r^2 + 4 + (z-1)^2}{4r} \right] - \frac{\sqrt{r}}{\sqrt{2}\pi} Q_{\frac{1}{2}} \left[\frac{r^2 + 4 + (z+1)^2}{4r} \right]. \quad (30)$$

The flux surfaces from the exact solution (Equation 30) are plotted in Figure 4. The developed code, with axisymmetric finite element, generates quite similar flux surfaces, as observed in Figure 5. The computation time for the axisymmetric finite element code has been about 110 seconds for over 5,000 nodes. The distribution of nodes was uniform on a simple rectangular grid. In comparison, the exact solution, as Equation 30, has needed about 28 and 14 seconds for elliptic integral and hyper-geometric series representations of the Legendre function, $Q_{\frac{1}{2}}(x)$.

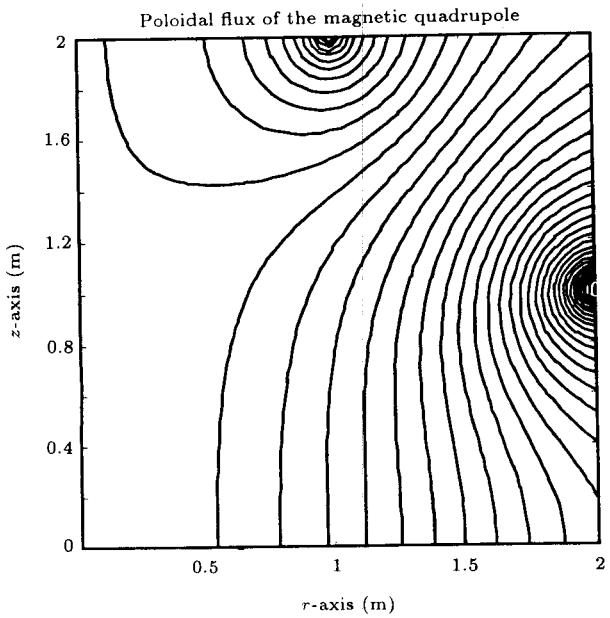

Figure 4. Exact poloidal flux contours of the magnetic quadruple as computed by the Green function technique.

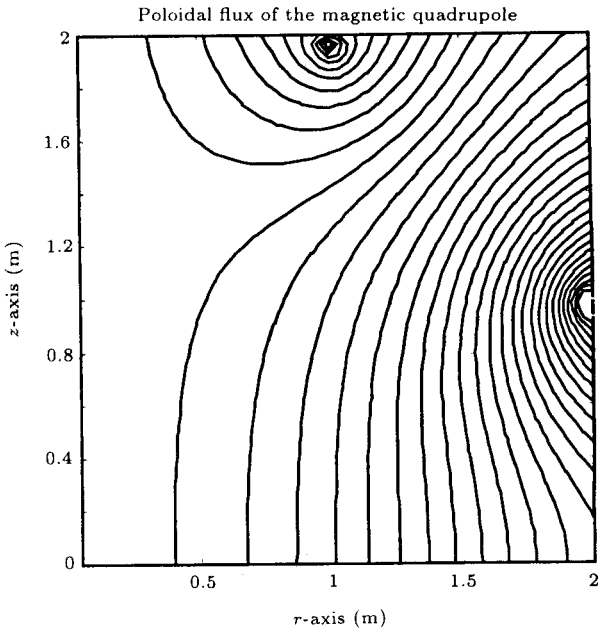

Figure 5. Poloidal flux contours of the magnetic quadruple as computed by the axisymmetric finite element code.

If the problem also involves point sources, then double integration, as suggested by Equation 16, is needed to find the exact solution. In this case, the efficiency of the Green function technique drastically diminishes, while the axisymmetric finite element code keeps to be as efficient as above.

The excellent efficiency of the code can be observed with the aid of Figure 6. Here, the computation time versus number of nodes is plotted. It can be easily detected that the algorithm complexity of the code has an order of roughly unity, that is, the computation

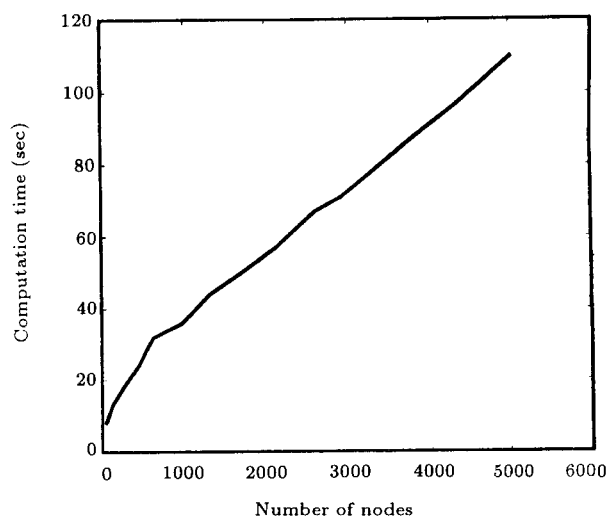

Figure 6. Computation time vs number of nodes, which grows almost linearly.

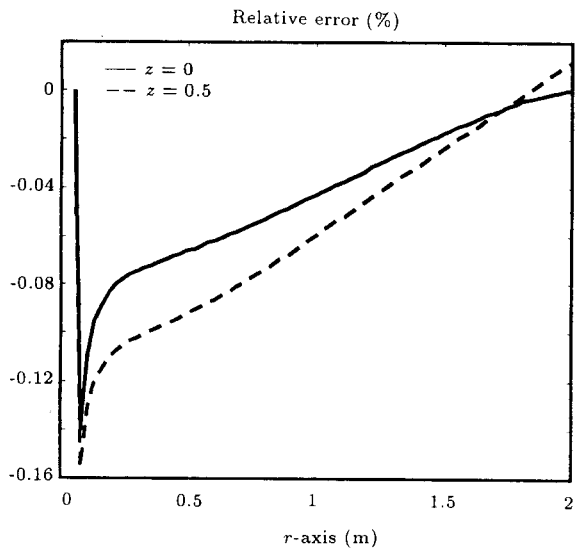

Figure 7. Error distribution profiles at $z = 0$ and $z = 0.5$.

time grows almost linearly with the dimension of the matrices or number of nodes.

In order to investigate the error distribution and behavior, two profiles of the relative error function at $z = 0$ and $z = 0.5$ have been plotted as shown in Figure 7. It can be observed that the error blows up near the z-axis, where $r = 0$. In order to have a lower computational error, it is, in general, thus, necessary to reduce the mesh size near the symmetry axis.

CONCLUSIONS

In this paper, an axisymmetric finite element method for computation of magnetic poloidal flux in axisymmetric magnetostatic machines was presented, which has been based on the variational formulation of the Grad-Shafranov equation. Inherent problems in the computation of magnetic flux by this method and proposed solution techniques to the difficulties were characterized. The code shows excellent efficiency and reasonable error distribution, as compared to the exact numerical methods.

REFERENCES

1. Zakharov, L.E. "Numerical methods for solving some problems of the theory of plasma equilibrium in toroidal configurations", *Nucl. Fusion*, **13**, pp 595-602 (1973).
2. Scheffel, J. "Linear MHD equilibria-exact and approximate solutions", *Internal Report TRITA-PFU-84-06, Department of Plasma Physics and Fusion Research*, Royal Institute of Technology, Stockholm (1984).
3. Zakharov, L.E. and Shafranov, V.D. "Equilibrium of current-carrying plasmas in toroidal configurations", in *Reviews of Plasma Physics*, **11**, Consultants Bureau, New York (1986).
4. Johnson, J.L., Dalhed, H.E., Greene, J.M., Grimm, R.C., Hsieh, Y.Y., Jardin, S.C., Manickam, J., Okabayashi, M., Stroder, R.G., Todd, A.M.M., Voss, D.E. and Weimerr, K.E. "Numerical determination of axisymmetric toroidal magnetohydro-dynamic equilibria", *J. Comput. Phys.*, **32**, pp 212-234 (1979).
5. Lao, L.L., Hirshman, S.P. and Wieland, R.M. "Variational moment solutions to the Grad-Shafranov equation", *Phys. Fluids*, **24**, pp 1431-1441 (1981).
6. Khait, V.D. "Variational method for approximately solving the problem of the MHD equilibrium of a Tokamak plasma", *Sov. J. Plasma Phys.*, **6**, pp 476-478 (1980).
7. Suzuki, Y. "Free-boundary MHD-equilibria in axisymmetric tori", *Nucl. Fusion*, **14**, pp 345-352 (1974).
8. Olson, R.E. and Miley, G.H. "An integral transform technique for solving the Grad-Shafranov equilibrium equation", *Trans. Am. Nucl. Soc.*, **39**, pp 489-490 (1981).
9. Ludwig, G.O. "Direct variational solutions to the Grad-Schlutter-Shafranov equation", Internal Report PPPL-3024, Princeton Plasma Physics Laboratory, Princeton (1994).
10. Fujii, N. and Hirai, M. "On the existence of a free boundary solution of the Grad-Shafranov equation", *J. Plasma Phys.*, **30**, pp 255-266 (1983).
11. Sawai, S., Tsuchimoto, M., Igarashi, H. and Honma, T. "Boundary element analysis of free boundary field-reversed configurations", *IEEE Trans. Magnetic*, **MAG-26**, pp 571-574 (1990).
12. Zienkiewics, O.C. and Taylor, R.L., *The Finite Element Method*, 4th Ed., McGraw-Hill, London (1988).
13. Sadiku, M.N.O., *Numerical Techniques in Electromagnetic*, CRC Press, Boca Raton (1992).
14. Gruber, R. and Rappaz, J., *Finite Element Method in Linear Ideal Magnetohydro-Dynamics*, Springer-Verlag, Berlin (1985).
15. Khorasani, S. "Green function of axisymmetric magnetostatics", *Proc. 9th Iranian Conf. on Elect. Eng.*, pp 4/0-4/5, Tehran (2001).
16. Amrollahi, R., Khorasani, S. and Dini, F. "Time-domain self consistent plasma equilibrium in Damavand Tokamak", *J. Plasma Fusion Res.*, **3**, pp 161-165 (2000).
17. Arfken, G., *Mathematical Methods for Physicists*, 3rd Ed., Academic Press, Orlando (1985).
18. Khorasani, S. and Rashidian, B. "A simple method for exact evaluation of element integrals in axisymmetric FEM", *Journal of Scientia Iranica*, **9**(4), pp 404-408 (2002).